Available online at www.sciencedirect.com
SCIENCE DIRECT®
Journal of Computational Physics 195 (2004) 1–16
JOURNAL OF COMPUTATIONAL PHYSICS
www.elsevier.com/locate/jcp

Second kind integral equations for the classical potential theory on open surfaces II

Shidong Jiang *,[1], Vladimir Rokhlin

Department of Computer Science, Yale University, New Haven, Connecticut 06520, USA

Received 11 July 2003; received in revised form 30 September 2003; accepted 1 October 2003

Abstract

A second kind integral equation formulation is presented for the Dirichlet problem for the Laplace equation in two dimensions, with the boundary conditions specified on a collection of open curves. The performance of the obtained apparatus is illustrated with several numerical examples. The formulation is a simplification of the equation previously constructed by the authors.

Keywords: Open surface problems; Laplace equation; Second kind integral equation; Dirichlet problem

AMS: 65R10; 77C05

1. Introduction

Integral equations have been one of principal tools for the numerical solution of scattering problems for more than 30 years, both in the Helmholtz and Maxwell environments. Historically, most of the equations used have been of the first kind, since numerical instabilities associated with such equations have not been critically important for the relatively small-scale problems that could be handled at the time.

The combination of improved hardware with the recent progress in the design of "fast" algorithms has changed the situation dramatically. Condition numbers of systems of linear algebraic equations resulting from the discretization of integral equations of potential theory have become critical, and the simplest way to limit such condition numbers is by starting with second kind integral equations. Hence, increasing interest in reducing scattering problems to systems of *second kind* integral equations on the boundaries of the scatterers.

* Corresponding author.
E-mail addresses: shidong@cs.yale.edu (S. Jiang), rokhlin@cs.yale.edu (V. Rokhlin).
[1] Supported in part by DARPA under Grant MDA972-00-1-0033, and by ONR under Grant N00014-01-1-0364.

0021-9991/$ - see front matter © 2003 Elsevier Inc. All rights reserved.
doi:10.1016/j.jcp.2003.10.001

During the last several years, satisfactory integral equation formulations have been constructed in both acoustic (Helmholtz equation) and electromagnetic (Maxwell's equations) environments, whenever all of the scattering surfaces are "closed" (i.e., scatterers have well-defined interiors, and have no infinitely thin parts). In this paper, we describe a second kind integral equation formulation for the Dirichlet problem for the Laplace equation with boundary data specified on a collection of "open" curves. We start with constructing the right inverse of the single layer potential operator on a line segment via simple analytic means; then we apply such operator as a preconditioner for the single layer potential operator on the curve considered to obtain a second kind integral operator.

Remark 1. In a recent paper [7], the authors construct a somewhat different procedure for the solution of problems of the classical potential theory with data specified on a collection of open surfaces. While the approach of the present paper is very similar to that of [7], in [7], the single layer potential is used to precondition the quadruple layer potential from the right; here, the quadruple layer potential is used to precondition the single layer potential from the right. For technical reasons, the latter leads to a drastically simplified numerical procedure (and also, requires simpler analysis); hence, this sequel to [7].

Remark 2. As observed by one of referees to this paper, a second kind integral equation is constructed in [11] (Chapter 16) in the Laplace environment. In [11], the solution of the Dirichlet problem is represented via the real part of the Cauchy's integral and the resulting boundary equation is a singular integral equation. A second kind integral equation is then obtained by applying the inverse operator of the Cauchy's integral operator from the left to both sides of the equation. However, the scheme of [11] cannot be easily extended either to three dimensions or to the Helmholtz equation in two dimensions, since it relies heavily on the harmonic property of the solution and the techniques of complex analysis.

Remark 3. As observed by another of referees to this paper, a closed surface enclosing very thin volumes presents difficulties closely related to those associated with open surfaces. This class of issues is not treated in this paper.

The layout of the paper is as follows. Section 2 contains an informal description of the procedure. In Section 3, the necessary mathematical and numerical preliminaries are introduced. In Sections 4, we present the principal analytic result of the paper. In Section 5, we describe a simple numerical implementation of the scheme. The performance of the algorithm is illustrated in Section 6 with several numerical examples. Finally, in Section 7 we discuss several generalizations of the approach.

2. Informal description of the procedure

In this section, we present an informal description of the procedure. We assume that $\gamma : [-1, 1] \to \mathbb{R}^2$ is a sufficiently smooth "open" (i.e., $\gamma(-1) \neq \gamma(1)$) curve with the parametrization

$$\gamma(t) = \widetilde{\gamma}\left(\frac{L}{2} \cdot (t+1)\right), \tag{1}$$

where L is the total arc length of the curve, and $\widetilde{\gamma} : [0, L] \to \mathbb{R}^2$ is the same curve parametrized by its arc length. The image of γ will be denoted by Γ. We consider the Dirichlet problem for the Laplace equation in two dimensions, with the boundary conditions specified on Γ, i.e.,

$$\begin{cases} \Delta u = 0 & \text{in } \mathbb{R}^2 \setminus \Gamma, \\ u = f & \text{on } \Gamma. \end{cases} \tag{2}$$

This problem has a unique bounded solution if the Dirichlet data f is sufficiently smooth (see, for example, [9, p. 121]). The purpose of this paper is to reduce the problem (2) to a second kind integral equation on Γ.

The tools of the classical potential theory by themselves do not lead to such an integral equation. Indeed, the standard prescription (see, for example, [9]) is to represent the solution of a Dirichlet problem by a *double* layer potential, and the solution of the Neumann problem by a *single* layer potential. In either case, the behavior of the singularity near the boundary is such that an integral equation of the second kind on Γ is obtained.

However, the classical procedure critically depends on Γ being a *closed* curve. Indeed, the potential of a double layer on the curve Γ experiences a jump when Γ is crossed; the magnitude of the jump is equal to the density of the double layer at the crossing point. This poses no problem when the curve is a closed one, since the potential is to be represented on only one (inner or outer) side of the curve. For an *open* curve, the potential has to be represented on both sides of the curve; and in most cases, the right-hand side f (viewed as the limiting value of the solution from both sides) has no jump across Γ. Thus, an attempt to represent the solution of (2) via a double layer potential results in a dipole density that is identically equal to zero.

One could attempt to represent the solution of (2) by a charge distribution on Γ. The resulting potential *is* continuous across Γ, and algorithms of this type have been constructed and used numerically (see, for example, [6]). However, the resulting integral equation is of the first kind (though, fortunately, with a logarithmically singular kernel), with all the usual numerical disadvantages. Another option is to use the quadruple layer potential of the form

$$R(\sigma)(x) = \int_{-1}^{1} \frac{\partial^2}{\partial N(t)^2} (\log ||x - \gamma(t)||) \cdot \sigma(t)\, dt, \tag{3}$$

with $N(t)$ the unit normal to Γ at $\gamma(t)$; the resulting equation is not an integral equation at all, containing a part that is actually a distribution. In engineering literature, such objects are known as "hypersingular integral equation". Satisfactory procedures have been constructed for their numerical solution (see, for example, [3,10,12]); however, these are not as simple or as stable as the many methods available for the solution of second kind integral equations.

This paper is based on the observation that when the curve is the line segment $I = [-1, 1]$, the right inverse of the single layer potential operator (denoted by S_I^{-1}) can be constructed by simple analytic means, where the single layer potential operator $S_I : L^1[-1, 1] \to C[-1, 1]$ is defined by the formula

$$S_I(\sigma)(x) = \int_{-1}^{1} \log |x - t| \cdot \sigma(t)\, dt. \tag{4}$$

Furthermore, if S_I^{-1} is used as a preconditioner for the single layer potential operator $S_\gamma : L^1[-1, 1] \to C(\mathbb{R}^2)$ on Γ defined by the formula

$$S_\gamma(\sigma)(z) = \int_{-1}^{1} \log |z - \gamma(t)| \cdot \sigma(t)\, dt, \tag{5}$$

i.e., the solution of the problem (2) is represented in the form

$$u(x) = S_\gamma \bigcirc S_I^{-1}(\eta)(x), \tag{6}$$

then the resulting boundary integral equation is of the *second kind*.

Remark 4. A stable second kind integral equation formulation has also been developed for the problem (2) in [7]. Two key observations used in [7] are: first, the product of the quadruple layer potential operator and the single layer potential operator is a second kind integral operator for the case of a closed curve; second, the case of a line segment can be solved analytically. The integral representation for the solution of the problem (2) in [7] is of the form

$$u(x) = Q_\gamma \bigcirc S_I \bigcirc (Q_I \bigcirc S_I)^{-1}(\eta)(x), \tag{7}$$

where Q_γ is the sum of a quadruple layer potential and a weighted double layer potential with the weight equal to the curvature, S_I is the single layer potential operator for the line segment $I = [-1, 1]$, and $(Q_I \bigcirc S_I)^{-1}$ is (in the appropriate sense) the right inverse of $Q_I \bigcirc S_I$. The approach of this paper differs from that of [7] in that the roles of Q and S are interchanged, leading to a simpler scheme. Indeed, straightforward analysis shows that the representation (6) is equivalent to

$$u(x) = S_\gamma \bigcirc Q_I \bigcirc (S_I \bigcirc Q_I)^{-1}(\eta)(x). \tag{8}$$

In other words, the solution of (2) is represented by a single layer potential on Γ preconditioned by the quadruple layer potential for the line segment I, with a further preconditioning by the right inverse of $S_I \bigcirc Q_I$ to eliminate the singularities at the end points.

3. Analytical preliminaries

In this section, we summarize several results from classical and numerical analysis to be used in the remainder of the paper. Detailed references are given in the text.

3.1. Chebyshev polynomials and Chebyshev approximation

Chebyshev polynomials are frequently encountered in numerical analysis. As is well known, Chebyshev polynomials of the first kind $T_n : [-1, 1] \to \mathbb{R}$ $(n \geqslant 0)$ are defined by the formula

$$T_n(x) = \cos(n \arccos(x)), \tag{9}$$

and are orthogonal with respect to the inner product

$$(f, g) = \int_{-1}^{1} f(x) \cdot g(x) \cdot \frac{1}{\sqrt{1 - x^2}}\, \mathrm{d}x. \tag{10}$$

Chebyshev polynomials of the second kind $U_n : [-1, 1] \to \mathbb{R}$ $(n \geqslant 0)$ are defined by the formula

$$U_n(x) = \frac{\sin((n + 1) \arccos(x))}{\sin(\arccos(x))}, \tag{11}$$

and are orthogonal with respect to the inner product

$$(f, g) = \int_{-1}^{1} f(x) \cdot g(x) \cdot \sqrt{1 - x^2}\, \mathrm{d}x. \tag{12}$$

The Chebyshev nodes x_i of degree N are the zeros of T_N defined by the formula

$$x_i = \cos \frac{(2i + 1)\pi}{2N}, \quad i = 0, 1, \ldots, N - 1. \tag{13}$$

For a sufficiently smooth function $f : [-1, 1] \to \mathbb{R}$, its Chebyshev expansion is defined by the formula

$$f(x) = \sum_{k=0}^{\infty} C_k \cdot T_k(x), \tag{14}$$

with the coefficients C_k given by the formulae

$$C_0 = \frac{1}{\pi} \int_{-1}^{1} f(x) \cdot T_0(x) \cdot (1 - x^2)^{-1/2} \, dx, \tag{15}$$

and

$$C_k = \frac{2}{\pi} \int_{-1}^{1} f(x) \cdot T_k(x) \cdot (1 - x^2)^{-1/2} \, dx, \tag{16}$$

for all $k \geqslant 1$. We will also denote by P_f^N the order $N - 1$ Chebyshev approximation to the function f on the interval $[-1, 1]$, i.e., the (unique) polynomial of order $N - 1$ such that $P_f^N(x_i) = f(x_i)$ for all $i = 0, 1, \ldots, N - 1$, with x_i the Chebyshev nodes defined by (13).

The following lemma provides an error estimate for the Chebyshev approximation (see, for example, [4]).

Lemma 5. *If $f \in C^k[-1, 1]$ (i.e., f has k continuous derivatives on the interval $[-1, 1]$), then for any $x \in [-1, 1]$,*

$$\left| P_f^N(x) - f(x) \right| = \mathrm{O}\left(\frac{1}{N^k} \right). \tag{17}$$

In particular, if f is infinitely differentiable, then the Chebyshev approximation converges superalgebraically (i.e., faster than any finite power of $1/N$ as $N \to \infty$).

3.2. Miscellaneous results

In this section, we collect several results from classical analysis to be used subsequently. Lemma 6 lists two standard definite integrals; both can be found (in a somewhat different form) in [5]. Lemma 7 states a standard fact from classical potential theory; it can be found in [9]. Finally, Lemma 8 states that if the curve γ is sufficiently smooth, then the restriction of the kernel of the operator $S_\gamma - S_I$ on Γ is also smooth (see (4), (5) for the definitions of S_I and S_γ).

Lemma 6. *For any $x \in (-1, 1)$,*

$$\int_{-1}^{1} \log |x - t| \cdot \frac{1}{\sqrt{1 - t^2}} \, dt = -\pi \cdot \log 2, \tag{18}$$

and

$$\text{p.v.} \int_{-1}^{1} \frac{1}{x - t} \cdot U_{n-1}(t) \cdot \sqrt{1 - t^2} \, dt = \pi \cdot T_n(x), \tag{19}$$

for any $n \geqslant 1$.

Lemma 7. *Suppose that $\gamma : [-1, 1] \to \mathbb{R}^2$ is a sufficiently smooth open regular curve with the parametrization (1), and that the function $\sigma \in L^1[-1, 1]$ satisfies the condition*

$$\int_{-1}^{1} \sigma(t) \, dt = 0. \tag{20}$$

Then the function $u : \mathbb{R}^2 \to \mathbb{R}$ defined by the formula

$$u(x) = \int_{-1}^{1} \log |x - \gamma(t)| \cdot \sigma(t) \, dt \tag{21}$$

is bounded in $\mathbb{R}^2$.

Lemma 8. *Suppose that $\gamma \in C^{k+1}[0,L]$ ($k \geqslant 1$) is an open regular curve parametrized by its arc length in $\mathbb{R}^2$. Suppose further that the function $r : [0,L] \times [0,L] \to \mathbb{R}$ is defined by the formula*

$$r(x,t) = \begin{cases} \log|\gamma(x) - \gamma(t)| - \log|x - t|, & x \neq t, \\ 0, & x = t. \end{cases} \tag{22}$$

Then $r \in C^k([0,L] \times [0,L])$.

Proof. Since γ is parametrized by its arc length, we have

$$|\gamma'(x)| = 1, \tag{23}$$

for all $x \in [0,L]$. Combining (22), (23), we observe that

$$r(x,t) = \log|h(x,t)|, \tag{24}$$

where the function $h : [0,L] \times [0,L] \to \mathbb{R}^2$ is defined by the formula

$$h(x,t) = \begin{cases} \frac{\gamma(x)-\gamma(t)}{x-t}, & x \neq t, \\ \gamma'(x), & x = t. \end{cases} \tag{25}$$

Obviously, h is k times continuously differentiable for $\gamma \in C^{k+1}[0,L]$ by Taylor's Theorem. Furthermore, since $\gamma(x) \neq \gamma(t)$ if $x \neq t$, and $|\gamma'(x)| = 1$ for all $x \in [0,L]$, we have

$$|h(x,t)| \neq 0 \quad \text{for all } (x,t) \in [0,L] \times [0,L]. \tag{26}$$

Therefore, the function $r = \log|h|$ is also k times continuously differentiable in $[0,L] \times [0,L]$. □

4. Analytical apparatus

4.1. Right inverse of the single layer potential operator on the line segment

The purpose of this section is Theorem 10, providing the right inverse of the single layer potential operator on the line segment $I = [-1,1]$. The construction is based on an elementary integral identity stated in Lemma 9.

Lemma 9. *For any $x \in (-1,1)$,*

$$\int_{-1}^{1} \log|x - t| \cdot \frac{T_0(t)}{\sqrt{1-t^2}}\,\mathrm{d}t = -\pi \cdot \log 2 \cdot T_0(x), \tag{27}$$

and

$$\int_{-1}^{1} \log|x - t| \cdot \frac{T_n(t)}{\sqrt{1-t^2}}\,\mathrm{d}t = -\frac{\pi}{n} \cdot T_n(x), \tag{28}$$

for any $n \geqslant 1$.

Proof. (27) directly follows from the combination of the identity (18) and the fact that $T_0(x) = 1$ for all $x \in [-1,1]$. To prove (28), we integrate by parts once, obtaining

$$\int_{-1}^{1} \log|x-t| \cdot \frac{T_n(t)}{\sqrt{1-t^2}}\,\mathrm{d}t = -\frac{1}{n}\,\mathrm{p.v.}\int_{-1}^{1} \frac{1}{x-t} \cdot U_{n-1}(t) \cdot \sqrt{1-t^2}\,\mathrm{d}t. \tag{29}$$

Now, (28) follows from the combination of (29), (19). □

Theorem 10. *Suppose that the linear operator* $\widetilde{S} : C[-1,1] \to L^1[-1,1]$ *is defined by its action on the functions* T_n $(n \geqslant 0)$ *via the formula*

$$\widetilde{S}(T_n)(x) = \begin{cases} -\dfrac{1}{\pi \cdot \log 2} \cdot \dfrac{T_0(x)}{\sqrt{1-x^2}}, & n = 0, \\ -\dfrac{n}{\pi} \cdot \dfrac{T_n(x)}{\sqrt{1-x^2}}, & n > 0. \end{cases} \tag{30}$$

Suppose further that the operator $S_I : L^1[-1,1] \to C[-1,1]$ *is defined by the formula*

$$S_I(\sigma)(x) = \int_{-1}^{1} \log|x-t| \cdot \sigma(t)\,\mathrm{d}t. \tag{31}$$

Then

$$S_I \circ \widetilde{S} = \mathscr{I}, \tag{32}$$

with $\mathscr{I}$ *the identity operator. In other words,* $\widetilde{S}$ *is the right inverse of* S_I *on the space of continuous functions.*

Proof. Since T_n $(n \geqslant 0)$ form a basis for the space $C[-1,1]$, and the operators S_I, $\widetilde{S}$ are linear, we only need to prove that the identity

$$S_I \circ \widetilde{S}(T_n)(x) = T_n(x) \tag{33}$$

holds for all $n \geqslant 0$. Substituting (30) into (31) we obtain

$$S_I \circ \widetilde{S}(T_n)(x) = \begin{cases} -\dfrac{1}{\pi \cdot \log 2} \cdot \displaystyle\int_{-1}^{1} \log|x-t| \cdot \frac{T_0(t)}{\sqrt{1-t^2}}\,\mathrm{d}t, & n = 0, \\ -\dfrac{n}{\pi} \cdot \displaystyle\int_{-1}^{1} \log|x-t| \cdot \frac{T_n(t)}{\sqrt{1-t^2}}\,\mathrm{d}t, & n > 0. \end{cases} \tag{34}$$

Combining (33), (34), we observe that it suffices to prove the identity

$$\int_{-1}^{1} \log|x-t| \cdot \frac{T_n(t)}{\sqrt{1-t^2}}\,\mathrm{d}t = \begin{cases} -\pi \cdot \log 2 \cdot T_0(x), & n = 0, \\ -\dfrac{\pi}{n} \cdot T_n(x), & n > 0, \end{cases} \tag{35}$$

which directly follows from Lemma 9. □

4.2. Second kind integral equation formulation

In this section, we reduce Problem (2) to an integral equation of the second kind on the curve Γ; the results are summarized in Theorem 12. We start with defining the operator $\widetilde{S}_\gamma : C[-1,1] \to C(\mathbb{R}^2)$ via the formula

$$\widetilde{S}_\gamma(\sigma)(z) = S_\gamma \circ \widetilde{S}(\sigma)(z), \tag{36}$$

with S_γ, $\widetilde{S}$ defined by (5), (30), respectively. Combining (36) with Theorem 10, we easily see that for arbitrary smooth $\sigma : [-1,1] \to \mathbb{R}$ and $\gamma(x) \in \Gamma$,

$$\widetilde{S}_\gamma(\sigma)(\gamma(x)) = S_I \circ \widetilde{S}(\sigma)(x) + (S_\gamma - S_I) \circ \widetilde{S}(\sigma)(\gamma(x)) = \sigma(x) + (S_\gamma - S_I) \circ \widetilde{S}(\sigma)(\gamma(x)), \tag{37}$$

and the following theorem shows that the operator $P_\gamma = (S_\gamma - S_I) \circ \widetilde{S}$ is compact.

Theorem 11. *Suppose that $\gamma : [-1,1] \to \mathbb{R}^2$ is a sufficiently smooth open regular curve with the parametrization* (1). *Suppose further that the operator $P_\gamma : C[-1,1] \to C[-1,1]$ is defined by the formula*

$$P_\gamma(\sigma)(x) = (S_\gamma - S_I)\bigcirc\widetilde{S}(\sigma)(\gamma(x)) = \int_{-1}^{1} (\log|\gamma(x) - \gamma(t)| - \log|x-t|) \cdot \widetilde{S}(\sigma)(t)\,\mathrm{d}t, \tag{38}$$

with S_γ, S_I, $\widetilde{S}$ defined by (5), (31), (30), *respectively. Then P_γ is compact.*

Proof. By Lemma 8, the function $\widetilde{r} : [-1,1] \times [-1,1] \to \mathbb{R}$ defined by the formula

$$\widetilde{r}(x,t) = \log|\gamma(x) - \gamma(t)| - \log|x-t| \tag{39}$$

is k times continuously differentiable for any $\gamma \in C^{k+1}[-1,1]$. Obviously, if $\widetilde{r}$ is expanded into a double Chebyshev series

$$\widetilde{r}(x,t) = \sum_{m=0}^{\infty}\sum_{n=0}^{\infty} K_{mn} T_m(x) T_n(t), \tag{40}$$

then there exists a positive number C such that

$$|K_{mn}| < \frac{C}{m^k \cdot n^k} \tag{41}$$

for any $m > 0$, $n > 0$. Now, for any $N > 0$, we will define the operator $P_N : C[-1,1] \to C[-1,1]$ by the formula

$$P_N(\sigma)(x) = \int_{-1}^{1} \widetilde{r}_N(x,t) \cdot \widetilde{S}(\sigma)\,\mathrm{d}t, \tag{42}$$

with the function $\widetilde{r}_N : [-1,1] \times [-1,1] \to \mathbb{R}$ defined by the formula

$$\widetilde{r}_N(x,t) = \sum_{m=0}^{N}\sum_{n=0}^{N} K_{mn} T_m(x) T_n(t). \tag{43}$$

Obviously, P_N is a compact operator since its range is of finite dimensionality. Furthermore, P_N converges to P_γ as $N \to \infty$ by (41). Hence, P_γ is also a compact operator.

We will represent the solution of Problem (2) via the formula

$$u(x) = \widetilde{S}_\gamma(\sigma)(x) + A = \int_{-1}^{1} \log|x - \gamma(t)| \cdot \widetilde{S}(\sigma)(t)\,\mathrm{d}t + A, \tag{44}$$

where A is a real constant to be determined. Combining Lemma 7 and Theorem 11, we obtain the principal result of this paper. □

Theorem 12. *Suppose that $\gamma : [-1,1] \to \mathbb{R}^2$ is a sufficiently smooth open regular curve with the parametrization* (1), *and that the function $f : [-1,1] \to \mathbb{R}$ is continuously differentiable. Suppose further that the continuous function $\sigma : [-1,1] \to \mathbb{R}$ and the coefficient A satisfy the equations*

$$\sigma(x) + P_\gamma(\sigma)(x) = f(x) - A, \tag{45}$$

$$\int_{-1}^{1} \sigma(x) \cdot \frac{1}{\sqrt{1-x^2}}\,\mathrm{d}x = 0, \tag{46}$$

with P_γ defined in (38). *Then the function $u : \mathbb{R}^2 \to \mathbb{R}$ defined by* (44) *is bounded in $\mathbb{R}^2$ and is the solution of the problem*

$$\begin{cases} \Delta u = 0 & \text{in } \mathbb{R}^2 \setminus \Gamma, \\ u = f & \text{on } \Gamma. \end{cases} \tag{47}$$

Remark 13. Obviously, the purpose of the constant A in the above theorem is to ensure the boundedness of the solution u of (2). In certain physical situations, the potentials of interest are not bounded at infinity, but rather grow logarithmically. In such cases, the solution to (2) assumes the form

$$u(x) = \widetilde{S}_\gamma(\sigma)(x), \tag{48}$$

with σ satisfying the integral equation

$$\sigma(x) + P_\gamma(\sigma)(x) = f(x). \tag{49}$$

5. Numerical algorithm

In this section, we construct a rudimentary numerical algorithm for the solution of the Dirichlet problem (47) via the Eqs. (45) and (46). Since the construction of the matrix and the solver of the resulting linear system are direct, the algorithm requires $O(N^3)$ work and $O(N^2)$ storage, with N the number of nodes on the boundary. While standard acceleration techniques (such as the Fast Multipole Method, etc.) could be used to improve these estimates, no such acceleration was performed, since the purpose of this section (as well as the following one) is to demonstrate the stability of the integral formulation and the convergence rate of a very simple discretization scheme.

By Theorem 12, the equations to be solved are (45) and (46), where the unknowns are the function σ and the real number A. To solve (45) and (46) numerically, we discretize the boundary into N Chebyshev nodes and approximate the unknown density σ by a finite Chebyshev series of the first kind,

$$\sigma(t) \simeq \sum_{k=0}^{N-1} C_k \cdot T_k(t), \tag{50}$$

with the coefficients C_k $(k = 0, \ldots, N-1)$ to be determined. In order to discretize (45), we start with observing that by (29), the action of the operator $\widetilde{S}$ on the function σ is described via the formula

$$\widetilde{S}(\sigma)(x) = \frac{1}{\sqrt{1-x^2}} \sum_{k=0}^{N-1} B_k \cdot C_k \cdot T_k(x), \tag{51}$$

where the coefficients B_k $(k = 0, \ldots, N-1)$ are given by the formulae

$$\begin{cases} B_0 = -\dfrac{1}{\pi \log 2}, \\ B_k = -\dfrac{k}{\pi}, \quad 1 \leqslant k \leqslant N-1. \end{cases} \tag{52}$$

Next, we approximate the kernel $\widetilde{r}(x,t)$ (see (40)) of the operator $S_\gamma - S_I$ with an expression of the form

$$\widetilde{r}(x,t) \simeq \sum_{i=0}^{N-1} \sum_{j=0}^{N-1} K_{ij} \cdot T_i(x) \cdot T_j(t). \tag{53}$$

Clearly, the coefficients K_{ij} have to be determined numerically, since the curve Γ is user-specified, and is unlikely to have a convenient analytical expression. Thus, we obtain the coefficients K_{ij} by first constructing the $N \times N$ matrix $R = (\widetilde{r}(x_i, t_j))$ $(i, j = 0, 1, \ldots, N-1)$ with x_i, t_j the Chebyshev nodes defined by (13) then converting R into the matrix $K = (K_{ij})$ $(i, j = 0, 1, \ldots, N-1)$ by the formula

$$K = U \cdot R \cdot U^T, \tag{54}$$

with $N \times N$ matrix $U = (U_{ij})$ defined by the formula

$$\begin{cases} U_{0j} = \frac{1}{N} \cdot T_0(x_j), & j = 0, 1, \ldots, N-1, \\ U_{ij} = \frac{2}{N} \cdot T_i(x_j), & i = 1, \ldots, N-1, \quad j = 0, 1, \ldots, N-1, \end{cases} \tag{55}$$

Finally, we approximate the prescribed Dirichlet data f by its Chebyshev approximation of order $N-1$

$$f(t) \simeq \sum_{k=0}^{N-1} \hat{f}_k \cdot T_k(t), \tag{56}$$

where the coefficients $\hat{f}_k$ can be obtained by first evaluating f at Chebyshev nodes x_i, then applying to it the matrix U defined by (55), i.e.,

$$\hat{f}_k = \sum_{i=0}^{N-1} U_{ki} \cdot f(x_i). \tag{57}$$

Combining (51), (53), (56),we discretize (45) into the equation

$$\widetilde{A} \cdot \begin{pmatrix} C_0 \\ C_1 \\ \vdots \\ C_{N-1} \end{pmatrix} + A \cdot \begin{pmatrix} 1 \\ \vdots \\ 0 \end{pmatrix} = \begin{pmatrix} \hat{f}_0 \\ \hat{f}_1 \\ \vdots \\ \hat{f}_{N-1} \end{pmatrix}, \tag{58}$$

with $N \times N$ matrix $\widetilde{A}$ defined by the formula

$$\widetilde{A} = I_N + K \cdot B, \tag{59}$$

with I_N the $N \times N$ identity matrix, and B the diagonal matrix defined by the formula

$$B_{ij} = B_i \cdot \delta_{ij}. \tag{60}$$

Furthermore, (46) leads to the equation

$$C_0 = 0, \tag{61}$$

Finally, (58) and (61) together form a linear system of dimension $N+1$ to be solved.

Remark 14. The generalization of the above scheme to the case of several disjoint open curves is straightforward, and has been implemented by the authors (see Example 4 in Section 6).

6. Numerical examples

A FORTRAN code has been written implementing the algorithm described in the preceding section. In this section, we demonstrate the performance of the scheme with several numerical examples. We consider

the problem in electrostatics: the boundary is made of conductor and grounded, the electric field incident on the boundary is generated by the sources outside the boundary. For these examples, we plot the equipotential lines of the total field and present tables showing the convergence rate of the algorithm.

Remark 15. In the examples below, the problems to be solved via the procedure of the preceding section have no simple analytical solution. Thus, we tested the accuracy of our procedure by evaluating our solution via the formula (44) at a large number M of nodes on the boundary Γ (in our experiments, we always used $M = 2000$), and comparing it with the analytically evaluated right-hand side. We did not need to verify the fact that our solutions satisfy the Laplace equation, since this follows directly from the representation (44).

In each of those tables, the first column contains the total number N of nodes in the discretization of each curve. The second column contains the condition number of the linear system. The third column contains the relative L^2 error of the numerical solution as compared with the analytically evaluated Dirichlet data on the boundary. The fourth column contains the maximum absolute error on the boundary. In the last two columns, we list the errors of the numerical solution as compared with the numerical solution with twice the number of nodes, where the solution is evaluated at 1000 equispaced points on a circle of radius 3.3 centered at the origin; the fifth column contains the relative L^2 error, and the sixth column contains the maximum absolute error.

Example 1. In this example, the boundary is the line segment parametrized by the formula

$$\begin{cases} x(t) = t, \\ y(t) = -0.2, \end{cases} \qquad -1 \leqslant t \leqslant 1. \tag{62}$$

The Dirichlet data are generated by a unit charge at $(0, 0)$. The numerical results are shown in Table 1. The source, curve and equipotential lines are plotted in Fig. 1.

Example 2. In this example, the boundary is a sinusoidal arc parametrized by the formula

$$\begin{cases} x(t) = 0.5t, \\ y(t) = \cos(t), \end{cases} \qquad -\frac{3\pi}{2} \leqslant t \leqslant \frac{3\pi}{2}. \tag{63}$$

The Dirichlet data are generated by one positive charge of unit strength at (0, 1.5) and another negative charge of unit strength at (0, 0). The numerical results are shown in Table 2. The sources, curve and equipotential lines are plotted in Fig. 2.

Table 1
Numerical results for Example 1

N	K	$E^2(\Gamma)$	$E^\infty(\Gamma)$	$E^2(u)$	$E^\infty(u)$
8	0.200E + 01	0.703E − 01	0.178E + 00	0.296E − 02	0.528E − 02
16	0.222E + 01	0.759E − 02	0.212E − 01	0.641E − 04	0.114E − 03
32	0.212E + 01	0.165E − 03	0.486E − 03	0.556E − 07	0.991E − 07
64	0.206E + 01	0.147E − 06	0.446E − 06	0.835E − 13	0.150E − 12
128	0.203E + 01	0.225E − 12	0.690E − 12	0.355E − 15	0.222E − 14
256	0.202E + 01	0.935E − 15	0.214E − 13	0.343E − 15	0.200E − 14

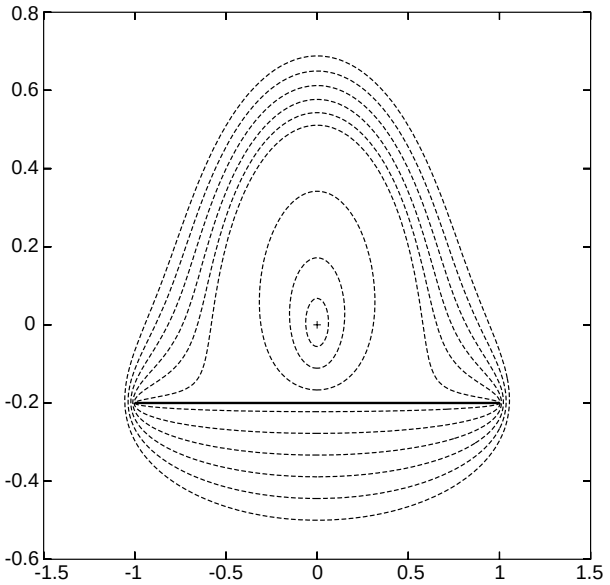

Fig. 1. Source, curve, and equipotential lines for Example 1.

Table 2
Numerical results for Example 2

N	K	$E^2(\Gamma)$	$E^\infty(\Gamma)$	$E^2(u)$	$E^\infty(u)$
32	0.195E + 01	0.271E − 01	0.864E − 01	0.658E − 02	0.469E − 02
64	0.187E + 01	0.240E − 02	0.847E − 02	0.146E − 03	0.104E − 03
128	0.182E + 01	0.422E − 04	0.157E − 03	0.135E − 06	0.955E − 07
256	0.179E + 01	0.307E − 07	0.117E − 06	0.245E − 12	0.173E − 12
512	0.178E + 01	0.431E − 13	0.160E − 12	0.971E − 15	0.133E − 14
1024	0.177E + 01	0.304E − 14	0.450E − 13	0.941E − 15	0.122E − 14

Example 3. In this example, the boundary is a spiral parametrized by the formula

$$\begin{cases} x(t) = t\cos(3.3\pi t) - 0.1, \\ y(t) = t\sin(3.3\pi t), \end{cases} \quad 0.2 \leqslant t \leqslant 3.2. \tag{64}$$

The Dirichlet data are generated by a unit charge at $(0, 0)$. The numerical results are shown in Table 3. The source, curve and equipotential lines are plotted in Fig. 3.

Example 4. In this example, we consider the case of several open curves. The boundary consists of three elliptic arcs parametrized by the formulae

$$\begin{cases} x_1(t) = -t\cos(3.3\pi t) - 1.45, \\ y_1(t) = -t\sin(3.3\pi t) + 0.55, \end{cases} \quad 0.2 \leqslant t \leqslant 1.2, \tag{65}$$

$$\begin{cases} x_2(t) = t\cos(3.3\pi t) - 0.1, \\ y_2(t) = t\sin(3.3\pi t) - 1.2, \end{cases} \quad 0.2 \leqslant t \leqslant 1.2, \tag{66}$$

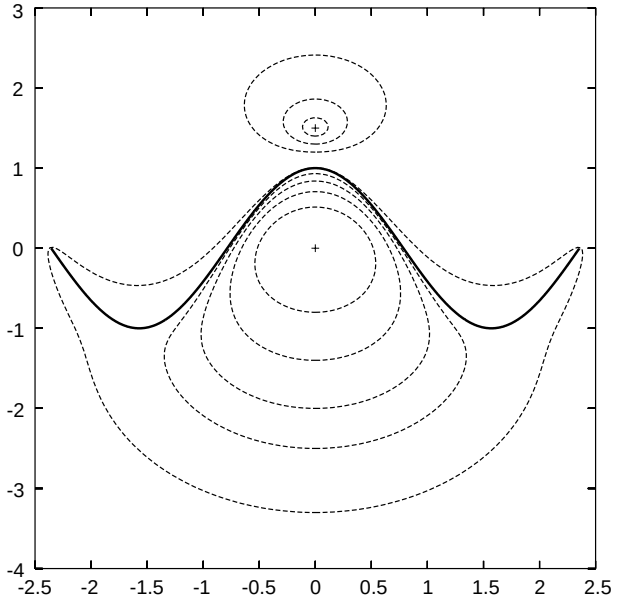

Fig. 2. Sources, curve, and equipotential lines for Example 2.

Table 3
Numerical results for Example 3

N	K	$E^2(\Gamma)$	$E^\infty(\Gamma)$	$E^2(u)$	$E^\infty(u)$
32	0.704E + 03	0.594E − 01	0.125E + 00	0.233E + 00	0.685E − 01
64	0.657E + 02	0.108E − 02	0.665E − 02	0.417E − 02	0.201E − 02
128	0.523E + 02	0.904E − 04	0.653E − 03	0.101E − 03	0.575E − 04
256	0.394E + 02	0.213E − 05	0.183E − 04	0.179E − 06	0.125E − 06
512	0.279E + 02	0.313E − 08	0.272E − 07	0.156E − 11	0.123E − 11
1024	0.196E + 02	0.184E − 13	0.147E − 12	0.211E − 13	0.933E − 14

$$\begin{cases} x_3(t) = t\cos(3.3\pi t) + 1.25, \\ y_3(t) = t\sin(3.3\pi t) + 0.85, \end{cases} \quad 0.2 \leqslant t \leqslant 1.2. \tag{67}$$

The Dirichlet data are generated by four unit charges located at $(0,0)$, $(1.35,0.75)$, $(-1.55,0.75)$, $(0,-1.2)$. The numerical results are shown in Table 4, where N is the number of nodes on each curve. The sources, curves and equipotential lines are plotted in Fig. 4.

Remark 16. The above examples illustrate the superalgebraic convergence of the scheme for smooth data and curves (see Lemmas 5, 8). The number of nodes needed depends on the complexity of the underlying geometry and the smoothness of the prescribed data. The condition number of the resulting linear system is usually very low.

7. Conclusions and generalizations

We have presented a second kind integral equation formulation for the Dirichlet problem for the Laplace equation in two dimensions, with the boundary condition specified on a curve (consisting of one or

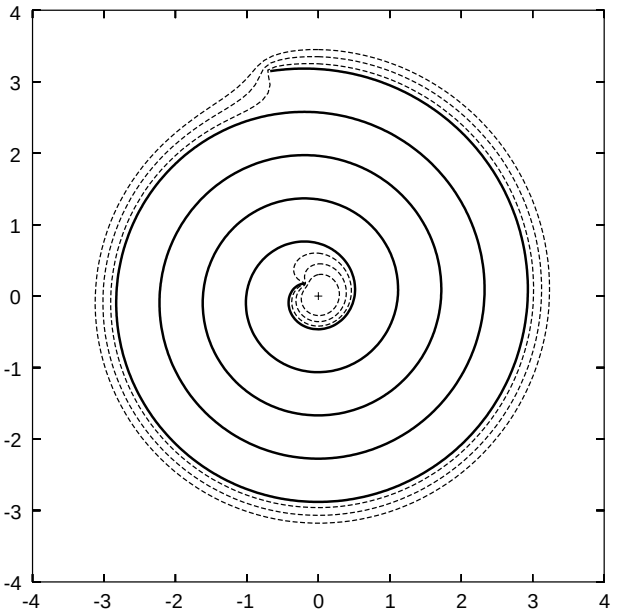

Fig. 3. Source, curve, and equipotential lines for Example 3.

Table 4
Numerical results for Example 4

N	K	$E^2(\Gamma)$	$E^\infty(\Gamma)$	$E^2(u)$	$E^\infty(u)$
8	0.204E + 02	0.825E − 01	0.370E + 00	0.848E + 01	0.451E − 01
16	0.183E + 02	0.180E − 01	0.121E + 00	0.259E + 00	0.121E − 02
32	0.145E + 02	0.183E − 02	0.131E − 01	0.665E − 03	0.355E − 05
64	0.116E + 02	0.355E − 04	0.455E − 03	0.738E − 07	0.252E − 09
128	0.963E + 01	0.314E − 07	0.353E − 06	0.302E − 11	0.232E − 13
256	0.851E + 01	0.511E − 13	0.520E − 12	0.269E − 11	0.192E − 13

more separate segments). The resulting numerical algorithm converges superalgebraically whenever both the boundary data and the curves are smooth.

In order to concentrate on the derivation and analysis of the integral formulation, we have chosen to use a very simple numerical scheme (see Section 5 above); the CPU time requirements of the procedure of Section 5 scale as n^3, with n the number of nodes in the discretization of the curve where the boundary condition is specified. A straightforward combination of the Fast Multipole Method (FMM), Fast Fourier Transform (FFT), and one of many standard iterative solvers yields an order $n \cdot \log(n)$ algorithm; such a scheme has been implemented, and will be reported at a later date. It is also possible to construct an order n scheme via the use of the FMM alone; according to the authors' estimates, for problems of practical size, this would offer no advantages over an FFT-based procedure.

Remark 17. In the iterative scheme outlined above, *each step* requires order $n \cdot \log(n)$ operations. Obviously, the complexity of the scheme also depends on the number of iterations needed to reach a required tolerance, which is to a large extent (though not entirely) determined by the spectral behavior of the discretized system. As observed by one of referees to this paper, a critical question for large-scale problems is

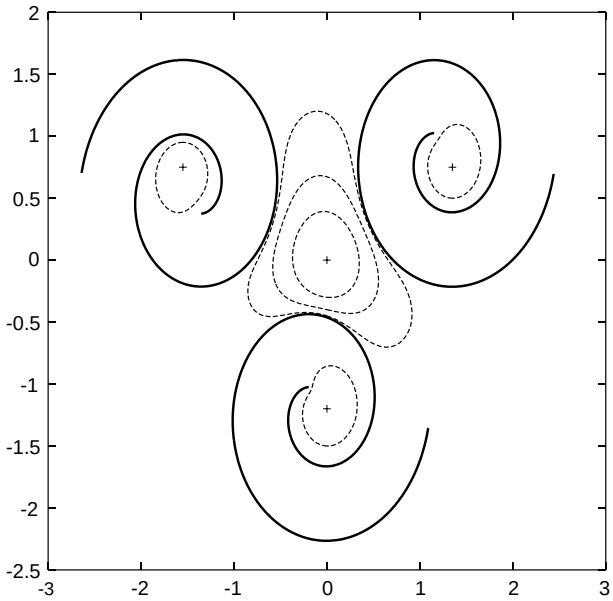

Fig. 4. Sources, curves, and equipotential lines for Example 4.

how the spectrum of the matrix A of the discretized system (or the spectrum of A^*A depending on the algorithm used) behaves as more and more reasonably separated curves of similar shapes are added to the geometry. This is currently under investigation.

The scheme of this paper can be applied almost without modification to elliptic PDEs other than the Laplace equation (such as Helmholtz equation, Yukawa equation, etc.). Indeed, the Green's function for any such equation has the form

$$G(x,y) = \phi(x,y) \cdot \log(||x-y||) + \psi(x,y), \tag{68}$$

with ϕ, ψ a pair of smooth functions (see, for example, [2]). When the procedure of Section 4 of this paper is applied to Green's function of the form (68), the result is unchanged, except for the change in the compact operator P_γ in (38). However, the convergence rate of the numerical scheme of Section 5 deteriorates drastically, since in this case the kernel K of the operator P_γ in (38) is logarithmically singular (while for the Laplace equation, it is smooth). High-order discretization schemes for such integral equations can be found in the literature (see, for example, [1,8,13]).

Finally, most results of this paper admit generalizations to two-dimensional surfaces in $\mathbb{R}^3$; while the necessary analytical apparatus is more involved, the results are very similar to those obtained here. Specifically, the product of a hypersingular integral operator on an open surface in $\mathbb{R}^3$ with the single layer potential operators (either from the left or from the right) is an integral operator of the second kind, except for simple corrections at the boundary of the surface. Such a scheme in three dimensions is being implemented, and will be reported at a later date.

Acknowledgements

The authors thank the referees of this paper for their helpful suggestions.

References

[1] B. Alpert, High-order quadratures for integral operators with singular kernels, J. Comput. Appl. Math. 60 (1995) 367–378.
[2] A. Friedman, Partial Differential Equations, Krieger, Huntington, 1976.
[3] J. Giroire, J.C. Nedelec, Numerical solution of an exterior Neumann problem using a double layer potential, Math. Comp. 32 (144) (1978) 973–990.
[4] D. Gottlieb, S.A. Orszag, Numerical Analysis of Spectral Methods: Theory and Applications, sixth ed., SIAM, Philadelphia, PA, 1993.
[5] I.S. Gradshteyn, I.M. Ryzhik, Table of Integrals, Series, and Products, fifth ed., Academic Press, New York, 1994.
[6] G.C. Hsiao, R.C. MacCamy, Solution to boundary value problems by integral equations of the first kind, SIAM Rev. 15 (1973) 687–705.
[7] S. Jiang, V. Rokhlin, Second Kind Integral Equations for Scattering by Open Surfaces I: Analytical Apparatus, Tech. Rep. Yale YALEU/DCS/TR-1233, Computer Science Department, Yale University, 2002.
[8] S. Kapur, V. Rokhlin, High-order corrected quadrature rule for singular functions, SIAM J. Numer. Anal. 34 (1997) 1331–1356.
[9] R. Kress, Linear Integral Equations, second ed., Springer, Berlin, 1999.
[10] M.N. Leroux, Equations Intégrales pour le probleme du potentiel életrique dans le plan, C. R. Acad. Sci. Paris Ser. Math. A 178 (1974) 541–544.
[11] N.I. Muskhelishvili, Singular Integral Equations, second ed., Dover, New York, 1992.
[12] J.C. Nedelec, Curved finite element methods for the solution of singular integral equations on surface in R^3, Comput. Meth. Appl. Mech. Eng. 8 (1974) 61–80.
[13] J. Strain, Locally corrected multidimensional quadrature rules for singular functions, SIAM J. Sci. Comput. 16 (1995) 992–1017.